ELSEVIER

Marine and Petroleum Geology 19 (2002) 951–970

Marine and Petroleum Geology

www.elsevier.com/locate/marpetgeo

Evidence of low flexural rigidity and low viscosity lower continental crust during continental break-up in the South China Sea

Peter Clift[a,*], Jian Lin[a], Udo Barckhausen[b]

[a]*Department of Geology and Geophysics, Woods Hole Oceanographic Institution, Woods Hole, MA 02543-1543, USA*
[b]*Bundesanstalt für Geowissenschaften und Rohstoffe, Stilleweg 2, D-30655 Hannover, Germany*

Received 10 June 2002; received in revised form 2 September 2002; accepted 19 September 2002

Abstract

The South China Sea was formed by seafloor spreading in the Late Oligocene at ~30 Ma following a series of extensional events within crust formed by Mesozoic continental arc. In this study, we interpreted faults along seismic reflection profiles from both the northern and southern conjugate margins of the South China Sea, and forward modeled these using a flexural cantilever model to predict modern basin geometries. When compared with the observed structure, the models based on upper crustal faulting consistently underpredicted the amount of subsidence, especially towards the continent–ocean transition (COT). We interpret this to indicate preferential extension of the continental lower crust along the COT on both margins, extending up to ~80 km landward from COT. The regional slope of the South China continental shelf indicates lower crustal viscosities of 10^{19}–10^{18} Pa s, representing an offshore continuation of the weak crust documented onshore on the eastern flanks of the Tibetan Plateau. Only in the region of Hainan Island in the western South China Shelf does lower crustal viscosity increase (10^{21}–10^{22} Pa s) and the preferential loss of lower crust become less pronounced and limited to <40 km from COT. This western area represents a rigid block analogous to the Sichuan Basin onshore.

Forward models based on upper crustal faulting support the idea of a very weak continental crust because models where the effective elastic thickness of the plate (T_e) exceeds 5 km fail to reproduce the geometry of the sub-basins within the Pearl River Mouth Basin (PRMB) of the South China Margin. The observed basins are too deep and narrow to be consistent with models invoking high flexural rigidity in the upper crust or mantle lithosphere. The fact that rifting and seafloor spreading seem to co-exist for ~5 my. adjacent to the PRMB is consistent with very weak continental crust during break-up.

Keywords: Flexure; Modeling; Stratigraphic

1. Introduction

Unlike the relatively well understood thermal and mechanical behavior of oceanic crust, the performance of continental crust during *deformation* remains a contentious issue because of the heterogeneous composition of the crust and the inheritance of tectonic and thermal characters from earlier deformation. Although plate tectonic theory initially suggested that both oceanic and continental crust deforms only along plate margins, there is now an understanding that continental crust can deform in a plastic or fluid fashion, far from plate boundaries, most notably in the Tibet-Himalaya orogen, where continued convergence between India and Asia has resulted in deformation extending >1000 km from the plate margin (England & Houseman, 1988).

In extensional systems a variety of modes of deformation of the continental crust are recognized, in part reflecting the mechanical strength of the lithosphere. Many non-volcanic margins, such as Iberia, Newfoundland, and southern Australia, are characterized by rotated basement fault blocks, wide zones of deformation extending more than 100 km from the continent–ocean transition (COT), and mantle peridotite exposures (Boillot, Beslier, Krawczyk, Rappin, & Reston, 1995). In contrast, volcanic margins, such as East Greenland, Norway, eastern US margin and NW Australia have sharp COTs and voluminous subaerially erupted basalts (Eldholm, Skogseid, Planke, & Gladczenko, 1995; Kelemen & Holbrook, 1995). Such different behavior of the crust under extension suggests either differing mechanical

* Corresponding author. Tel.: +1-508-289-3437; fax: +1-508-457-2187.
E-mail address: pclift@whoi.edu (P. Clift).

0264-8172/02/$ - see front matter © 2002 Elsevier Science Ltd. All rights reserved.
PII: S0264-8172(02)00108-3

strengths in the plate, and/or different rates of extension (Buck, 1991). Although Karner & Watts (1982) proposed that the flexural rigidity of continental margins is low during active extension and then increased with time after that ceases, the strength of continental crust during the rift–drift transition has remained a matter of controversy. Subsidence evidence from many sedimentary basins suggests that flexural strength during extension must have been low (Barton & Wood, 1984; Bellingham & White, 2000; Fowler & McKenzie, 1989; Watts, 1988). While some workers have argued for a weak continental lithosphere with strength located principally in a brittle, relatively thin, upper crust layer (Maggi, Jackson, McKenzie, & Priestley, 2000), others have invoked significant flexural strengths in rift zones (Ebinger, Bechtel, Forsyth, & Bowin, 1989; Van der Beek, 1997; Weissel & Karner, 1989), based on gravity studies of the flexural wavelength around the rift, as well the presence of seismic activity deep in the plate (Foster & Jackson, 1998; Jackson & Blenkinsop, 1993). A general division can be made between the rifting of thermally mature, cratonic continental lithosphere and hot, young, orogenic or subduction-altered crust, representing strong and weak end members, respectively.

Here we examine a type example of rifting within arc-type crust, within the South China Sea. We examine the basin geometry and subsidence patterns in order to assess the patterns of strain accommodation within the plate on both conjugate margins. We use subsidence modeling to constrain the flexural rigidity of the plate during extension, and its relationship to the crust of neighboring SE Asia.

2. Geologic setting

The South China Sea was formed by oceanic spreading along a WSW–ENE axis during the Oligo-Miocene during magnetic anomaly Chron 11 (~30 Ma) in the eastern part of the basin (Briais, Patriat, & Tapponnier, 1993; Lu, Ke, Wu, Liu, & Lin, 1987; Taylor & Hayes, 1980). The origin of the extensional forces is controversial and lies outside the study presented here. Extension in the area is believed to have started in the Late Cretaceous–Early Paleocene (Schlüter, Hinz, & Block, 1996), and seems to have exploited the location of a pre-existing Andean-type arc, located above a north-dipping subduction zone along the south coast of China (Hamilton, 1979; Jahn, Chen, & Yen, 1976). U–Pb dating of the arc volcanic and intrusive rocks exposed in Hong Kong (Davis, Sewell, & Campbell, 1997) indicates that magmatic activity ceased after 140 Ma, although $^{40}Ar/^{39}Ar$ ages of granites from the Pearl River Mouth Basin (PRMB) also suggest that some magmatism continued into the Late Cretaceous–Paleocene (Lee et al., 1999). Thus, because 80 my is the approximate duration for continental lithosphere to regain thermal equilibrium after a tectonic or thermal event (McKenzie, 1978), the Paleocene activity implies that rifting in South China Sea affected lithosphere that was hotter and weaker than equilibrium.

Coring at ocean drilling program (ODP) Site 1148 near the COT (Fig. 2) shows that, following earlier smaller extensional events, extension was active in that location during the Late Oligocene and that bathyal water depths (>500 m) existed along the COT at the time of break-up (Clift, Lin, & ODP Leg 184 Scientific Party, 2001; Wang et al., 2000). Subsidence modeling in the South China Sea is complicated by the existence of significant topography along the margin prior to Oligocene extension. Drilling on the Reed Bank adjacent to the Dangerous Grounds margin (Fig. 1), which forms the conjugate to the PRMB, has identified deep-water, clastic sedimentary rocks of pre-Middle Eocene age (Taylor & Hayes, 1980), indicating that there was a deep marine trough in that region at that time. The situation is further complicated by the collision of the southern Dangerous Grounds shelf with Borneo and Palawan, resulting in a partially filled flexural trough along the south edge of that shelf (Hinz & Schlüter, 1985). Subsidence related to this collisional deformation needs to be removed from that resulting from the Oligocene extension for that latter event to be understood.

3. Previous work

A number of different tectonic models have been invoked to account for the extension leading to break-up along the South China margin. While Schlüter et al. (1996) have argued for the activity of both simple and pure shear extension at different times during the break-up of the margin, Su, White, & McKenzie (1989) favored a pure shear model to explain subsidence in the PRMB. Hayes et al. (1995) identified major normal faults located close to the COT that appeared to penetrate the entire crust and suggested a weak crust that may have been entirely brittle, at least during the final stages of break-up in this area. Clift & Lin (2001) used a one-dimensional back-stripping subsidence analysis of well data from the PRMB to suggest moderate preferential mantle over crustal extension for that margin. Clift et al. (2001) employed an instantaneous two-dimensional forward modeling approach for interpreted reflection seismic profiles across the PRMB, Beibu Gulf Basin and Nan Con Som Basin (Fig. 1) to suggest that those basins that directly abutted the oceanic crust of the deep basin here have preferentially experienced lower crustal extension along that contact. However, lack of data from both margins prevented an investigation of whether a loss of lower crust had occurred on both conjugate margins in that study.

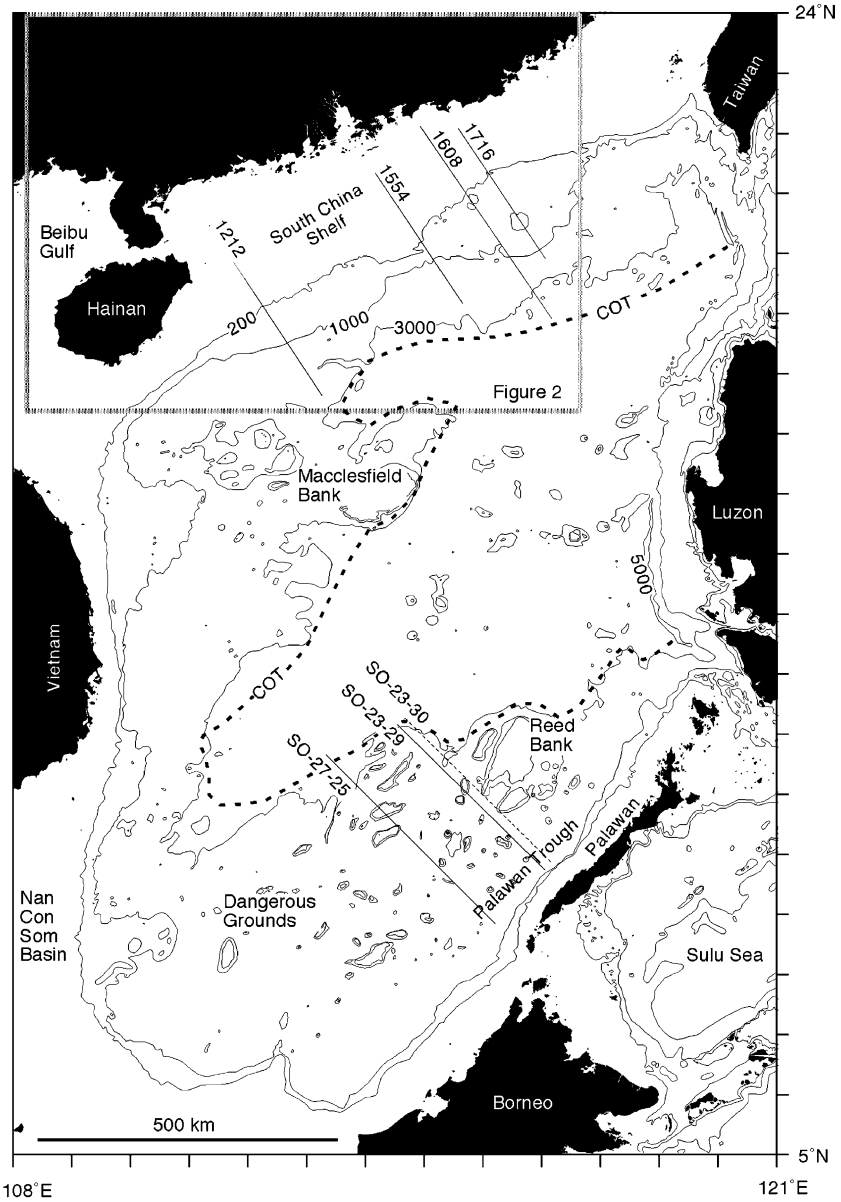

Fig. 1. Bathymetric map of the South China Sea showing the principle geologic and physical features that define the basin, together with the locations of multichannel seismic data considered in this study. COT, continent–ocean transition. Water depths in meters.

Lithgow-Bertelloni & Gurnis (1997) have suggested that southeast Asia is underlain by a region of cold, dense mantle asthenosphere formed by long-lived subduction in the western Pacific. This material is sinking deep into the upper mantle, causing dynamic subsidence, so that sediment-loading corrected depths to basement are as much as 1 km shallower than might be predicted from simple stretching models. However, Wheeler & White (2000) calculated the depth to basement in the region and after removing the effects of lithospheric extension and cooling, compared this prediction with that derived from Lithgow-Bertelloni and Gurnis (1997) model. They concluded that basin formation was largely controlled by rift tectonics and that dynamically driven subsidence due to subduction is not a factor in the South China Sea.

In this study we extended the previous subsidence analysis by examining for the first time structural transects through opposing conjugate margins using a two-dimensional subsidence analysis technique (Clift et al., 2001).

4. Data sources

The subsidence analysis performed in this study is based on seismic data from across the South China Shelf (Fig. 2) and Dangerous Grounds (Fig. 1). These data were released by

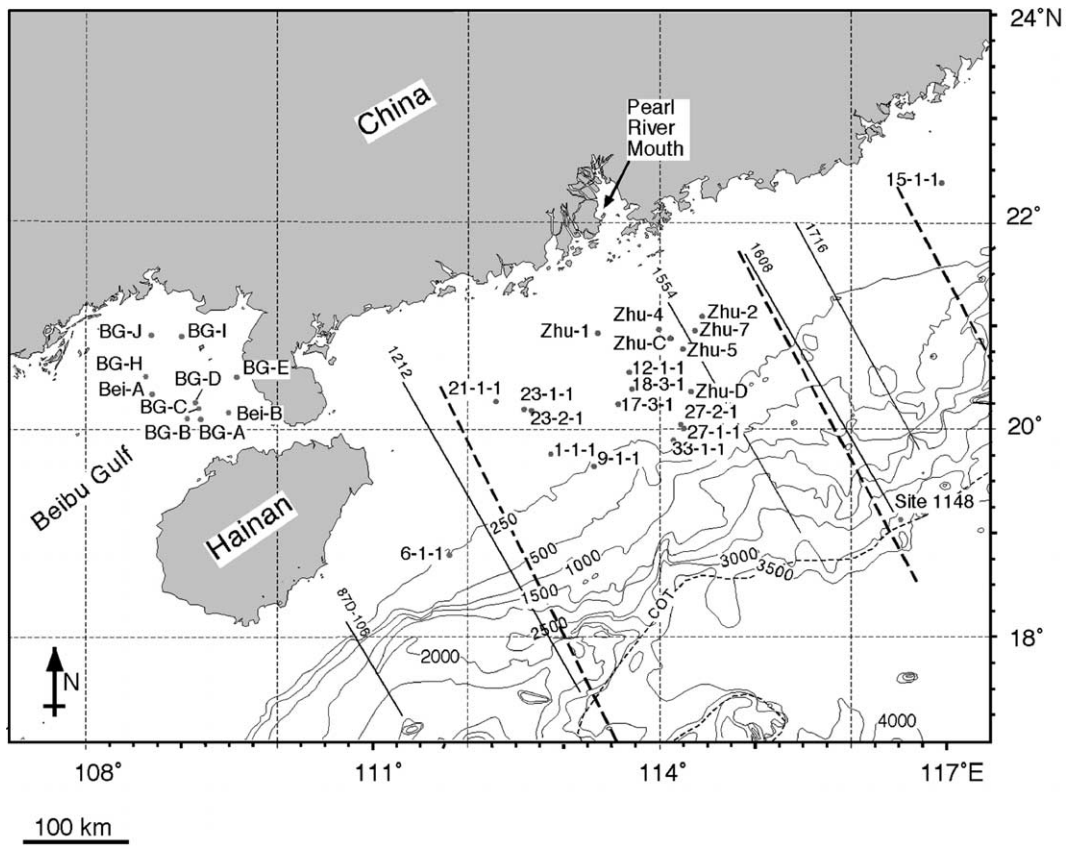

Fig. 2. Detailed bathymetric map of the South China Shelf and Beibu Gulf to show the location of the seismic profiles considered in this study, the location of the seismic refraction profiles of Nissen et al. (1995), shown in bold dashed lines, and the drilling sites mentioned in the text. Water depths in meters.

agreement with the Chinese National Offshore Oil Company (CNOOC), British Petroleum (BP Exploration plc), the Philippine Department of Energy and the German Federal Institute for Geosciences. The seismic data are of multi-channel reflection type, usually 96 channel, and were collected by a variety of different contractors mostly in 1979 and 1980. Most but not all of the data were depth migrated during processing using the stacking velocities. Only paper copies of the processed lines were available for use in this study. The original data are not presented here because at the scale of reproduction possible no crucial features would be discernable. Although the stratigraphy of the PRMB is well known, that on the Dangerous Grounds is poorly known and for the purpose of this work we simply divide the stratigraphy into seismically-defined pre-rift, syn-rift and post-rift units. The division between syn- and post-rift is the most important and is defined as those layers that show clear growth into a fault zone, rather than draping geometries. The age of the cessation of rifting is taken as 25 Ma from the published well data from the PRMB (Clift & Lin, 2001; Su et al., 1989), and from ODP Site 1148 (Wang et al., 2000). Although the basin was extended again at ~14 Ma (Clift & Lin, 2001) this was a minor event compared to the Oligo-Miocene break-up and did not generate significant accommodation space.

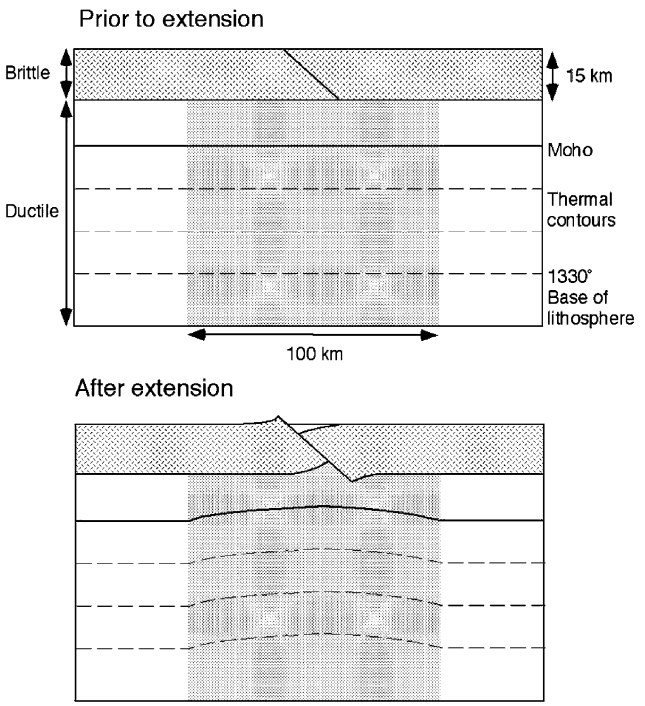

Fig. 3. A schematic representation of the flexural-cantilever model for lithospheric deformation showing assumptions of simple shear faulting in the brittle upper crust and the assumed same amount of pure shear in the lower crust and mantle (redrawn from Kusznir et al. (1991)).

5. Flexural modeling based on measured upper crustal extension

We have investigated the structure of the continental shelf and COT along a series of transects on both PRMB and Dangerous Grounds margins. We employ the flexural cantilever model of Kusznir, Marsden, and Egan (1991) to model the deformation and subsidence that would result from the extension measured from normal faults identified on seismic profiles (Fig. 3). In this approach we make no attempt to replicate the basin morphology, but simply extend continental lithosphere using the faults seen on the seismic profiles and then predict what sort of basin this would form after 25 my of post-rift subsidence. The synthetic basin produced is based only on the flexural cantilever model and the recognized extension across the faults seen on the profiles. Misfits between model and observation can thus be used to describe how the actual deformation in the ductile lower crust and mantle differed from the uniform pattern assumed by the model and calculated from the brittle extension in the upper crust.

Five transects, 1212, 1554 and 1716 from the South China Shelf and Lines SO-27-25 and SO-23-29 from the Dangerous Grounds, were chosen because of their substantial length across the shelf and on to the continental slope (Figs. 4–8). Line 1212 was chosen because it lies close to one of the seismic refraction profiles of Nissen et al. (1995), while Line 1554 was chosen so that results from the flexural model can be compared with the results of Clift and Lin (2001) backstripping work on the industrial wells centered in the PRMB (Fig. 2). Line 1716 allows changes in deformation along the margin to be traced further east than

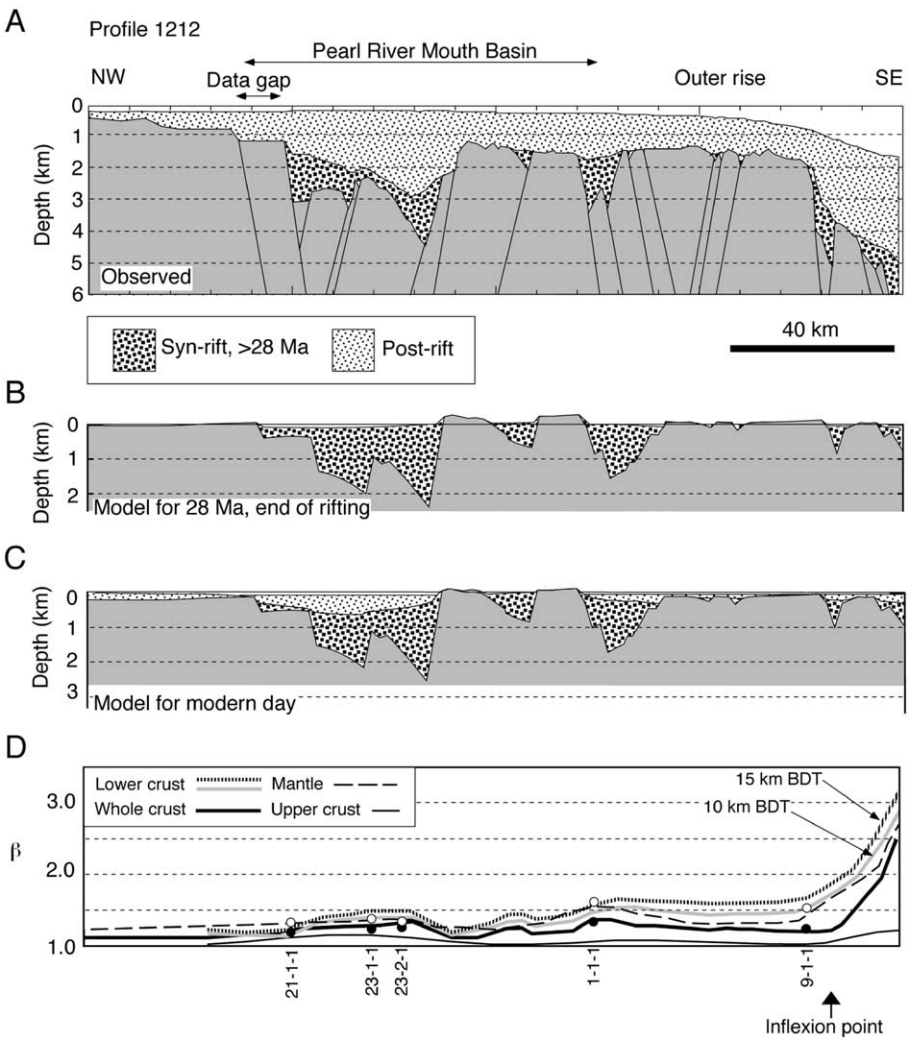

Fig. 4. (A) Interpreted seismic section crossing the PRMB long profile 1212. See Fig. 2 for location. Interpreted horizons are the pre-rift crystalline basement, the top of the syn-rift and the seafloor. (B) Forward model predicted by the flexural cantilever model of Kusznir, Marsden and Egan (1991), resulting from extension along the faults interpreted from the seismic profiles and assumed ductile flow in the lower crust and mantle. Sedimentation is set to fill the basin to 100 m of water; $T_e = 3$ km; Erosion = 80% of subaerial topography (C) Forward model showing predicted post-rift sedimentation after 28 my. (D) Lateral variations in the predicted extension for the whole crust, upper crust, lower crust assuming 15 km deep brittle–ductile transition, lower crust for 10 km deep transition and mantle lithosphere. Solid dots and open circles represent estimates of crustal and mantle extension derived from nearby wells (Clift & Lin, 2001) and projected on to the line of section.

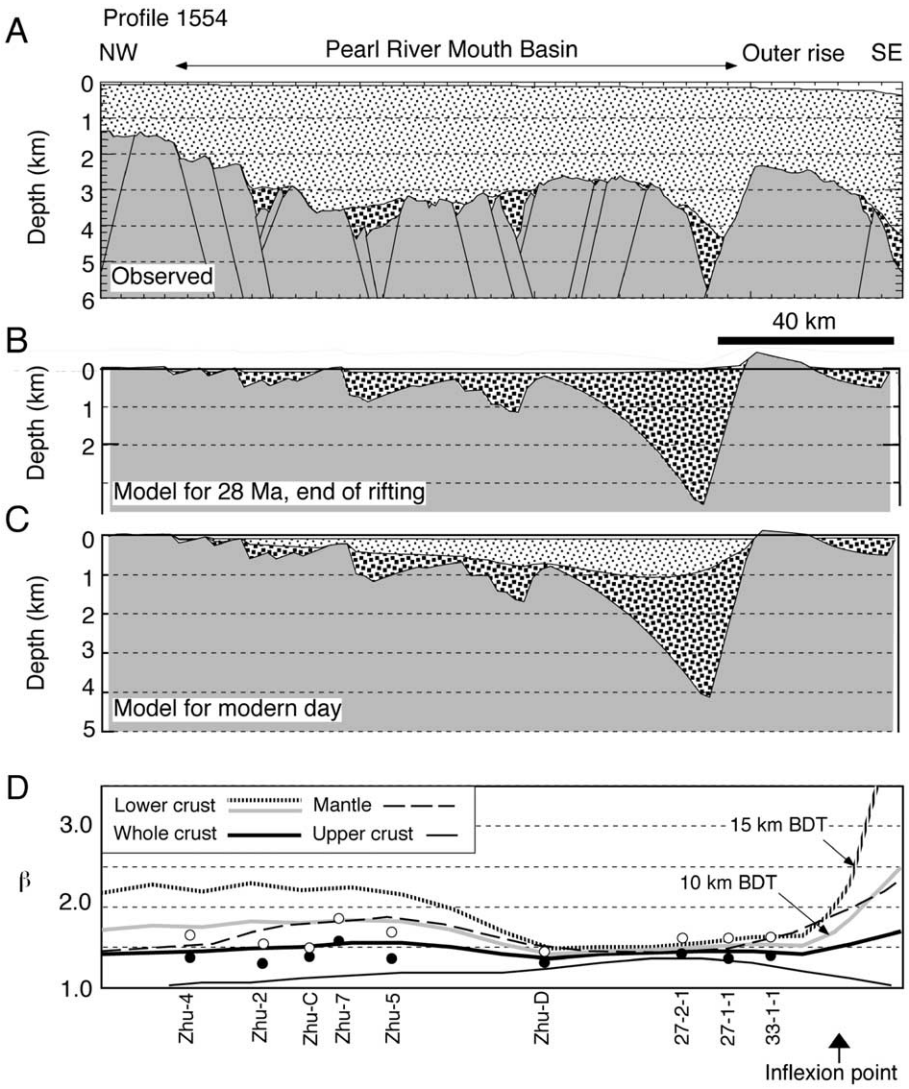

Fig. 5. Profile 1554. See Fig. 3 for explanation.

Line 1608, which was modeled in a similar fashion by Clift et al. (2001).

Although the profiles often continue as far as COT, the lack of data below 5 s two-way-time meant that the reflection data was no longer imaging the top of the basement in the outer part of the margin, making extension estimates impossible. Consequently, we focus our basin modeling efforts on those portion of the profiles that cross the shelf and upper slope.

We estimate the extension due to the faulting seen on the seismic profiles by measuring not only the dip of each fault, but also its heave (i.e. the horizontal extension across the fault). Examples of the quality of the seismic data used are shown in Fig. 9. Because of the difficulty of reproducing entire profiles at a scale that is useful to the reader, we here show examples from Profile 1716 showing the nature and extent of faulting along part of that profile located close to the coast (Fig. 9(A) and (B)), as well as over the outer structural high (Fig. 9(C) and (D)), where no faulting is apparent.

The flexural cantilever model of Kusznir and Egan (1989) and Kusznir, Roberts, and Morley (1995) assumes the deformation of the plate being divided between a brittle upper crust, where simple shear along discrete faults is the prime mode of strain accommodation, and a ductile lower crust and mantle deforming in a sinusoid pure shear mode (Fig. 3). Although a sinusoid is a simplification of the strain distribution, this assumption does mimic the expected strain distribution over long wavelengths in a plastic lower lithosphere. The flexural cantilever model defines the base of the lithosphere to be at the 1330 °C isotherm, with a thickness of 125 km prior to extension. The model also assumes instantaneous extension. Application of this analytical method to rift systems, such as the North Sea (Roberts, Yielding, Kusznir, Walker, & Dorn-Lopez, 1993) and East Africa (Kusznir et al., 1995), as well as passive margin basins (e.g. Jeanne D'Arc basin, Kusznir & Egan, 1989) has achieved good matches of the rift architecture and sedimentary fill, allowing the lateral variability in extension to be modeled (Kusznir et al., 1995).

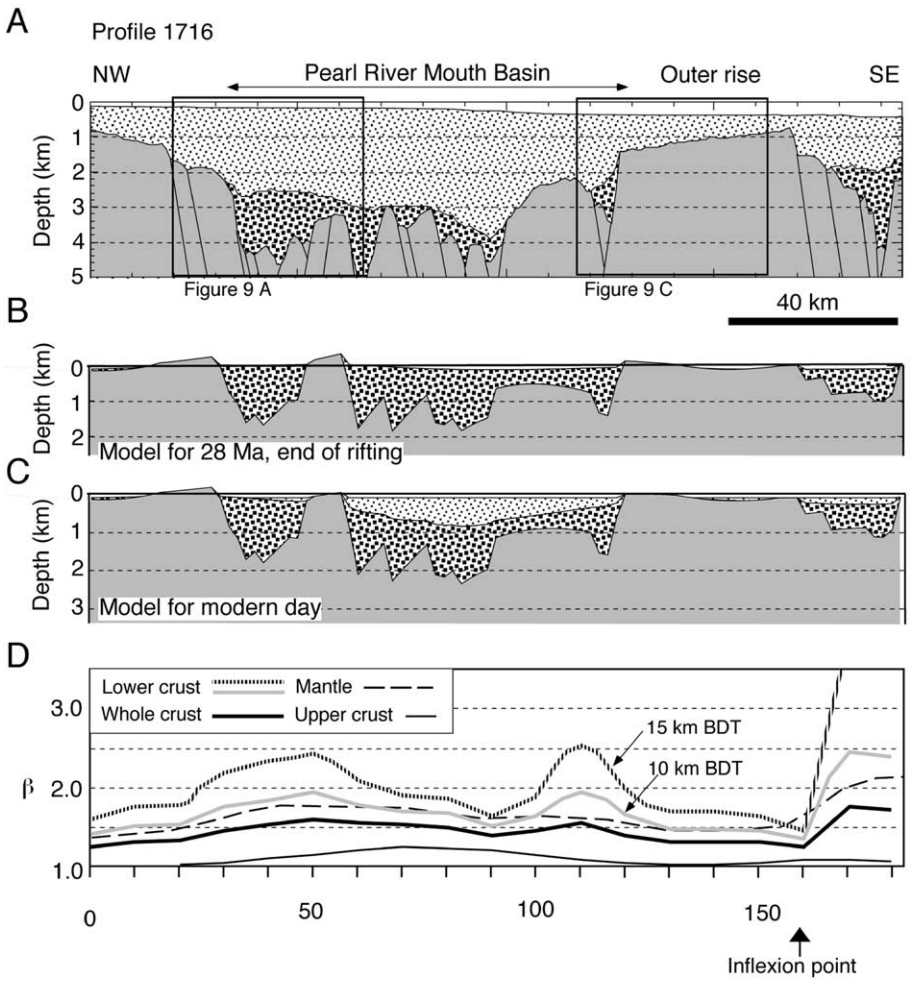

Fig. 6. Profile 1716. Boxes in (A) show the locations of detailed seismic data shown in Fig. 9 See Fig. 3 for explanation.

5.1. Flexural rigidity

The flexural strength of the lithosphere is considered to lie at the top of the plate in this extensional model. We choose an effective elastic thickness (T_e), of 3 km for our forward models. In terms of estimating the total amount of subsidence that would be generated through extension along the identified faults, the results presented here will be substantially correct regardless of the precise T_e chosen for this region, although the basin geometries will differ with T_e. To determine the effect of T_e on the fault-generated topography we use profile 1554 as an example. A series of forward models of the profile were generated using a range of T_e 1, 3, 5, 10 and 15 km but the same degree of extension (Fig. 10). Although the total subsidence predicted by all the profiles is lower than that observed, it is clear is that as T_e increases the ability of the forward model to reproduce the observed basement geometry on the scale of individual half graben declines. In particular, we note that while the observed basement geometry is marked by deep, narrow half graben, those models in which T_e is large are incapable of matching this, because of the need to compensate extension over broad regions. Forward modeling therefore supports the use of a T_e value of 1–3 km in the South China Sea during active extension, based on the ability to reproduce the basement geometry on the scale of individual half graben.

The modern flexural rigidity of the Dangerous Grounds margin can be estimated through consideration of the flexural trough (Palawan Trough) formed by the collision of that margin with the Palawan and Borneo active margin to the south. Loading of the southern edge of the Dangerous Grounds has created a flexural trough whose geometry is controlled by the modern flexural rigidity (Figs. 7 and 8). Because of the thermal recovery of the mantle lithosphere since the end of extension, the modern value of T_e must represent a maximum for the syn-rift value. Greater values for T_e result in wider flexural basins with greater degrees of uplift in the flexural forebulge. Determining the size of the flexural forebulge is difficult in this setting because of the amplitude of the rifted basement topography compared to the size of the forebulge. The section for profile SO-23-30 published by Hinz and Schlüter (1985) shows that there is no appreciable forebulge uplift in this area, implying very low T_e for the modern Dangerous Grounds. The width of the flexural trough at ~50 km can be used to calculate the T_e

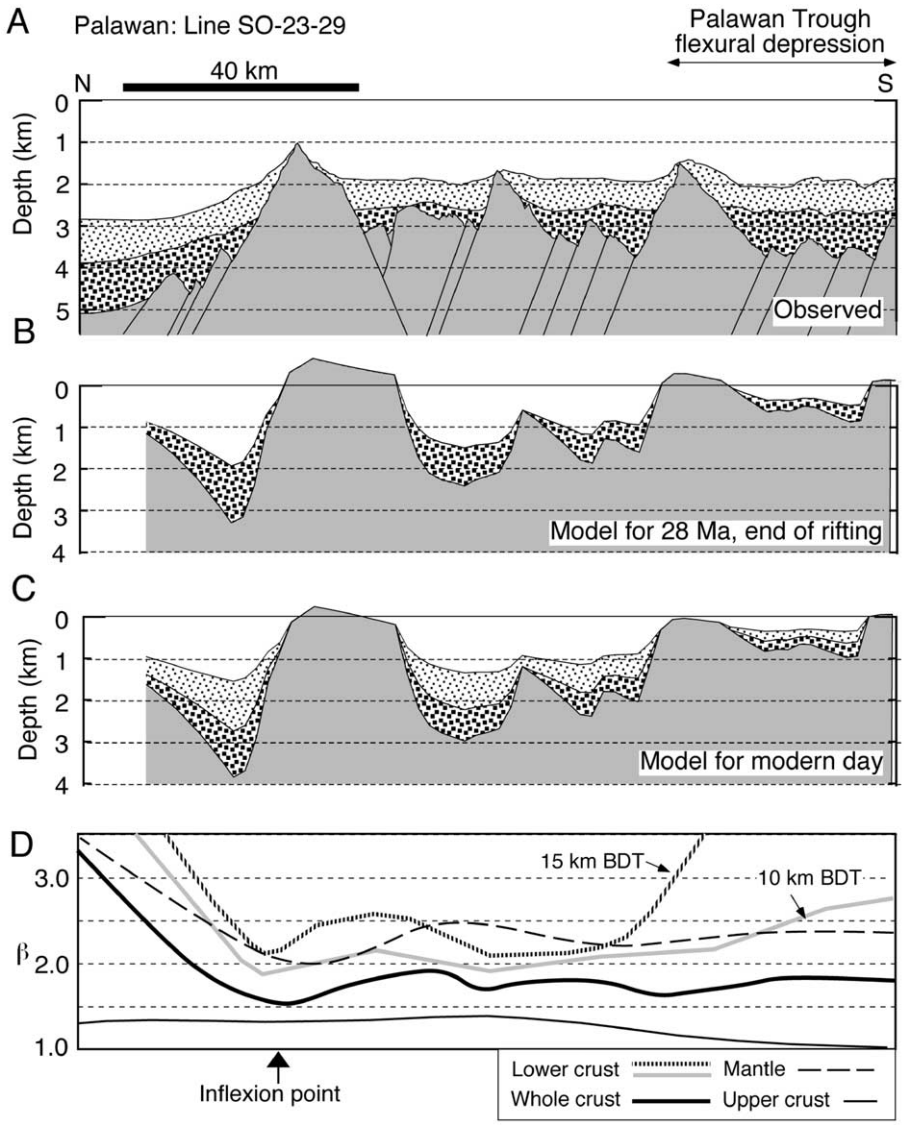

Fig. 7. Profile SO-23-29. See Fig. 3 for explanation. Note that no dated wells lie close to this profile, so that the stratigraphy can only be divided in pre-, syn- and post-rift.

using a simple flexural model, yielding a value of ~8–10 km for the modern plate. Karner and Watts (1982) demonstrated that older passive margins have higher values of T_e and inferred that margins strengthen through time. T_e was thus likely less than 8–10 km during the rifting, consistent with the low values used in the forward models presented here.

In a similar fashion Lin and Watts (2002) have used the flexure of the South China margin under the Taiwan fold and thrust belt to estimate flexural rigidity at the extreme eastern edge of the Chinese margin. Their study yielded modern T_e values for the South China margin of 13 km in that area. Following the same argument used in the Dangerous Grounds, the syn-rift values for T_e would be <13 km, and thus potentially compatible with the 1–3 km estimated from the PRMB, or the <8–10 km in the Dangerous Grounds. White (1999) noted that for rifts where extension exceeded 30% T_e ranged from 1 to 11 km, with a mode of 5–6 km. In the subsequent modeling, we use a uniform T_e of 3 km as a reference for all profiles. The T_e of 3 km used here is more than 1–2 km estimated from the Basin and Range (Buck, 1988) and is comparable to 3 km estimated for East Africa (Kusznir et al., 1995). We emphasize that although the predicted basin geometries on the scale of individual half graben will differ for different T_e, our main conclusions on the importance of lower crust and upper mantle ductile flow can be reached using higher assumed T_e values.

5.2. Other evidence for low strength in the south china lithosphere

The flexural cantilever model has been criticized by some workers for underpredicting the elastic thickness of

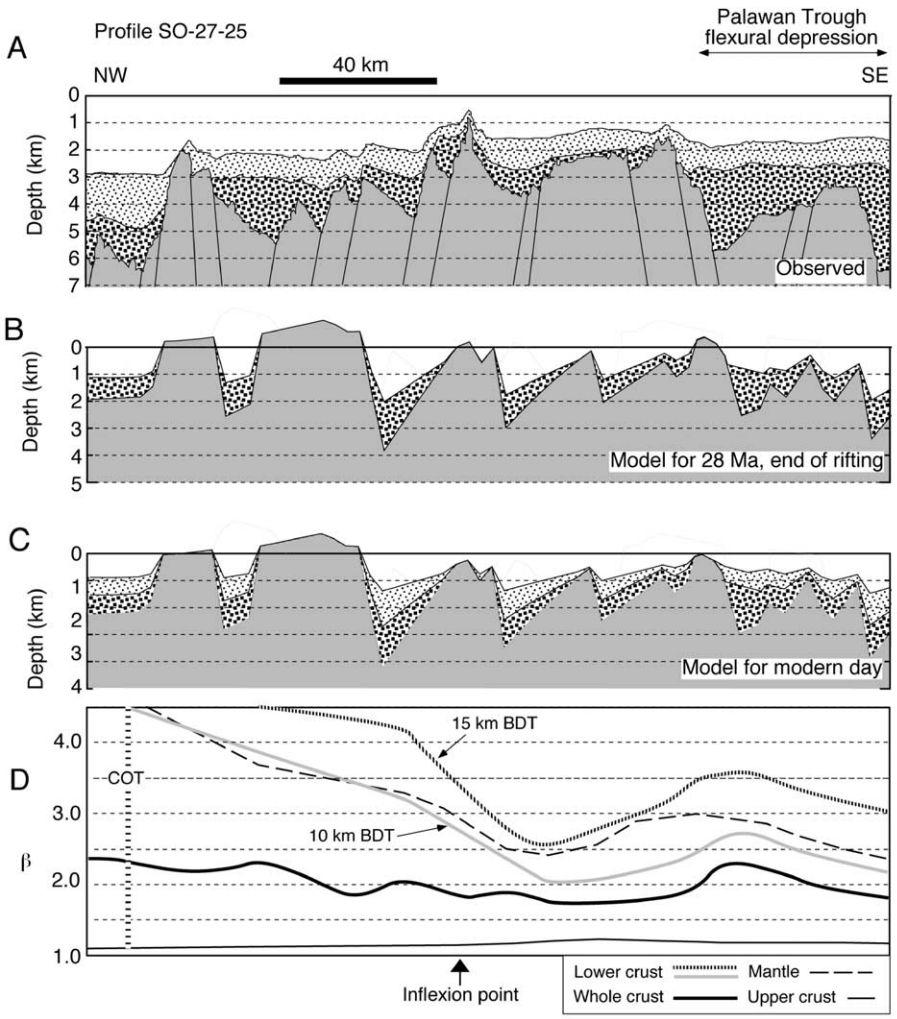

Fig. 8. Profile SO-122-25. See Fig. 3 for explanation. Note that no dated wells lie close to this profile, so that the stratigraphy can only be divided in pre-, syn- and post-rift.

the continental crust compared to estimates based on gravity and seismic data, and for over-estimating the amount of rift flank uplift, most notably in the Baikal Rift (van der Beek, 1997). Van der Beek (1997) instead argues in favor of either crustal necking models, such as that employed on the Gabon margin by Watts and Stewart (1998), or detachment faulting models as being better predictors of the extensional deformation of the continental crust. However, because necking models do not incorporate faulting they cannot account for the footwall uplift of individual faults, and consequently tend to underpredict rift flank topography (Roberts & Kusznir, 1998).

The sharp change from a brittle upper crust to a ductile lower crust that characterizes the flexural cantilever model provides a reasonable simulation of the rapid drop in mechanical strength with depth predicted for a quartz-dominated crust. Such a strength drop is a consequence of increasing in temperature with depth resulting in a change in the style of crustal deformation from brittle failure above to creep below (Carter, 1976). However, as noted by van der Beek (1998), the model does not account for upper mantle strength and so is least applicable to rifts in cold cratonic areas (e.g. Baikal, East Africa) and works best in areas where the strength in the lithosphere is focused in the crust (e.g. Aegean Sea, Western USA; Maggi et al., 2000). In the case of the South China margin, the tectonic setting, coupled with what we know of the flexural strength, support the idea of strength being concentrated in the upper brittle part of the plate (Maggi et al., 2000). In particular, the fact that the rift exploits a recently active arc would suggest that the mantle lithosphere in this area would be thin and weak due to the residual heat (Draut, Clift, Hannigan, Layne, & Shimizu, 2002). The presence above a subduction zone also allows the possibility of trace amounts of volatiles derived from the oceanic slab. The presence of even low percentages of water in the mantle is known to significantly reduce the mantle viscosity (Hirth & Kohlstedt, 1996), reducing the ability of that level of the plate to support flexural loads. The arc

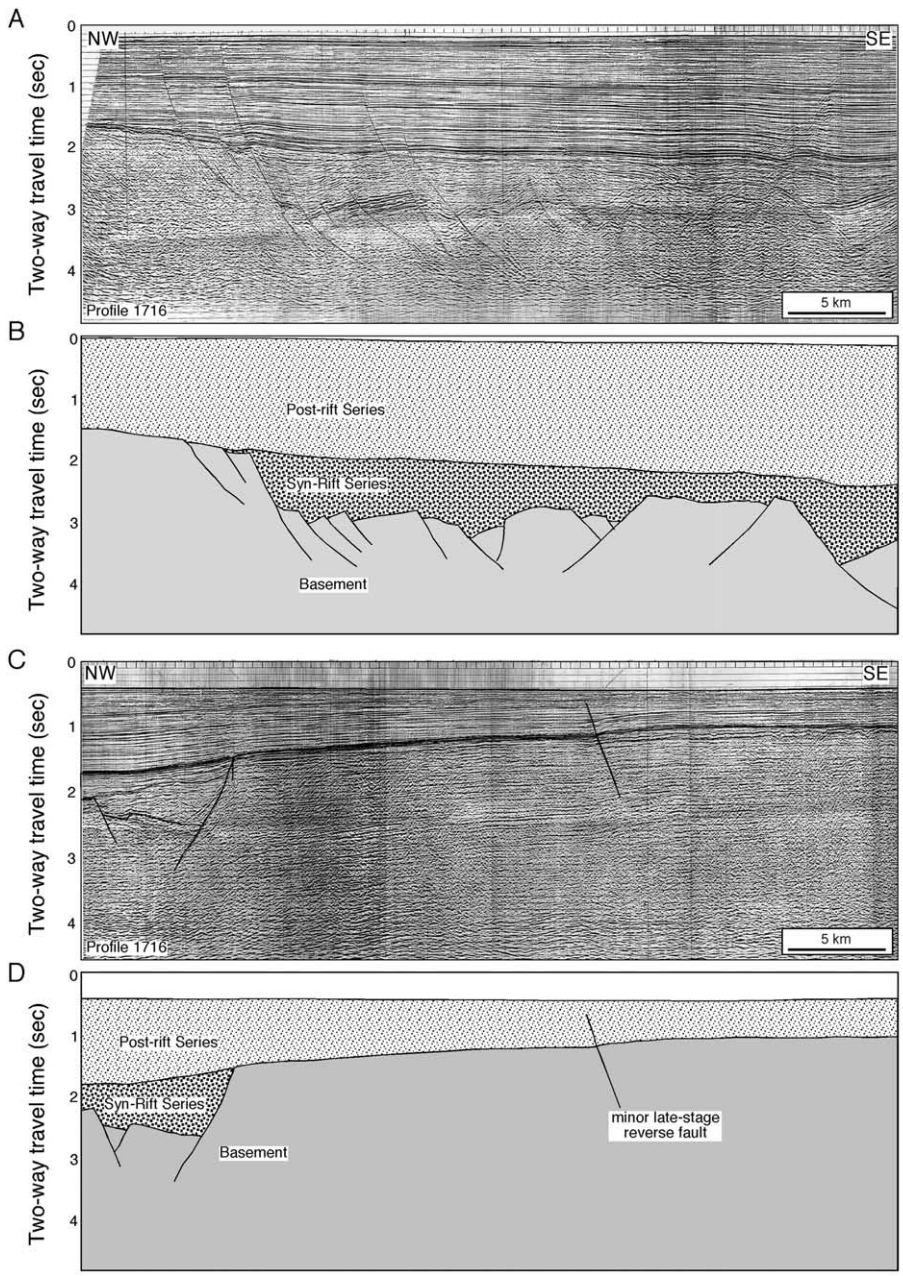

Fig. 9. Examples of the seismic data used to make the sections shown in Figs. 4–8. (A) Landward portion of Profile 1716, with (B) interpreted section. The lack of obvious faulting across the outer structural high is shown in (C) the original reflection data and (D) the interpreted section, also along Profile 1716.

setting is in stark contract to the dry, and strong olivine rheology known from oceanic lithosphere (Kohlstedt & Goetze, 1974).

Although the basin geometries indicate low T_e values during and after rifting it can be argued that these values might reflect strength in the upper crust only, with the influence of a strong mantle lithosphere being hidden by detachment between the two in the weak lower crust. However, recent finite element modeling of extending continental lithosphere now suggests that for most geological environments the brittle upper crust does not behave independently of the mantle lithosphere, regardless of the strength of the lower crust (Behn, Lin, & Zuber, 2002). This implies that the basin geometries seen around the South China Sea reflect the total strength of the lithosphere, and not just a weak upper crustal layer acting independently of a strong mantle lithosphere. The low T_e values implied by the forward modeling (Fig. 10) thus account for the strength in the mantle, as well as the crust, and constrains the entire plate to being weak during continental break-up.

Further support for the use of low values of T_e is provided by two-dimensional inverse modeling of the basin stratigraphy in the central PRMB by Bellingham and White (2000). In this approach the age structure and thickness of the stratigraphy was used to estimate

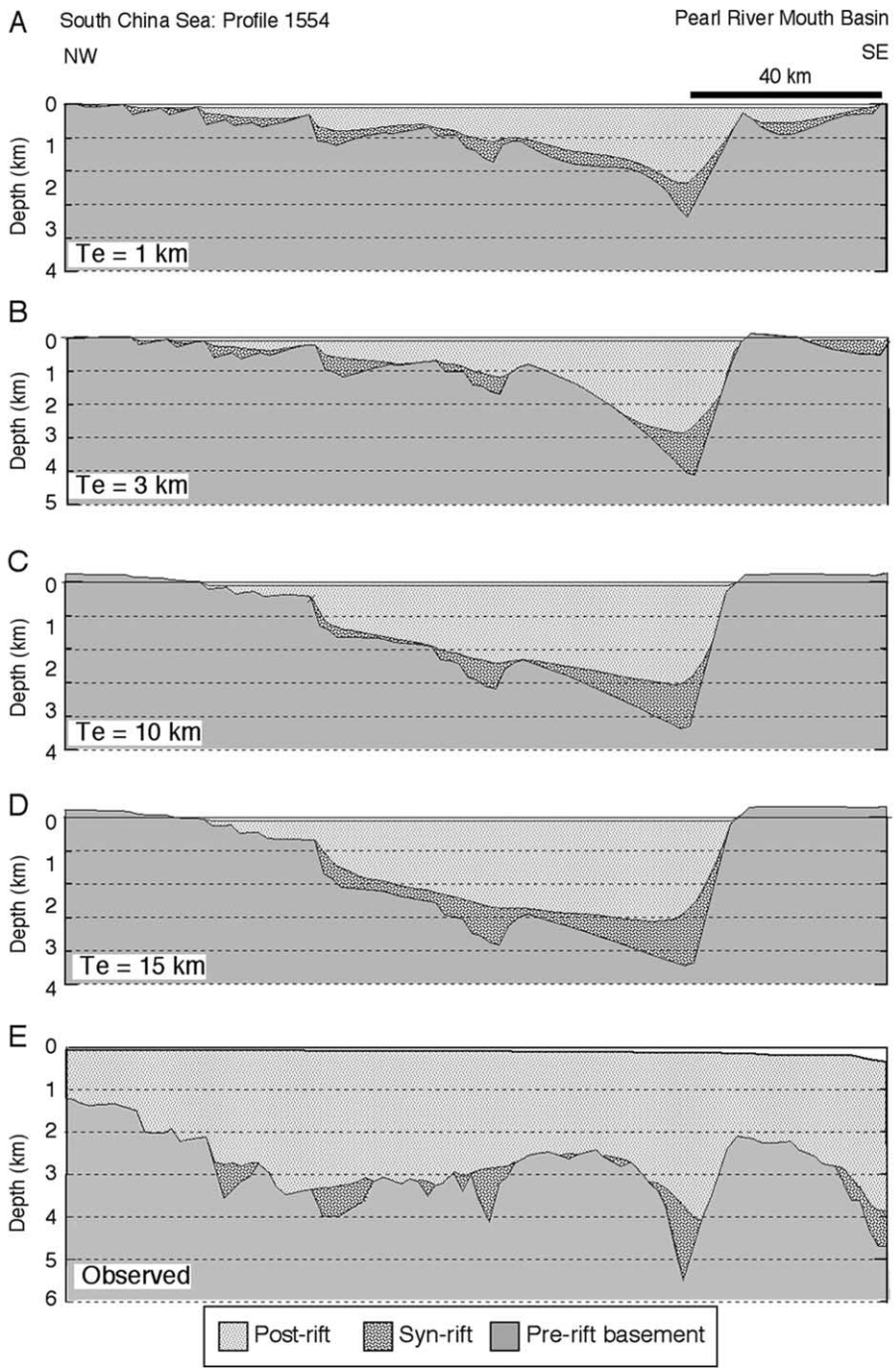

Fig. 10. Forward flexural-cantilever model of profile 1554 28 my after rifting showing sensitivity of the model to variations in elastic thickness (A) $T_e = 1$ km, (B) $T_e = 3$ km, (C) $T_e = 10$ km, (D) $T_e = 15$ km, (E) modern interpreted structure.

temporal and lateral variations in strain rate. The inverse solutions were seen to be most geologically realistic when T_e values close to zero were used. With higher T_e values anomalous periods of extension are predicted for which no other geologic or geophysical evidence exists. We conclude that T_e in the South China Sea probably did not exceed 3–5 km during the main Oligocene phase of extension.

5.3. Limitations of crustal ductile deformation in models

The flexural cantilever model assumes the same amount of ductile extension in the lower crust and mantle lithosphere as there is brittle extension in the upper crust. The model distributes the ductile deformation in a sinusoidal fashion over any given wavelength, typically 100 km, below the brittle–ductile transition (Fig. 3; Kusznir

et al., 1991). The 100 km wavelength is preferred because widths of 75–150 km are required to produce forward models that match the observed basin geometries and stratigraphies in most rifts. Observations in the Gulf of Suez rift demonstrate regional doming due to mantle lithosphere extension which is significantly broader than the narrow zone of faulting in the rift axis. Such a model implies a depth of total crustal necking in the middle of the crust at <15 km. This necking depth is shallower than the values of 15–20 km that has been used in rifted margin settings to explain the seismically-determined shape of the Moho and the size of the rift flank uplift (Janssen, Torne, Cloetingh, & Banda, 1993; Kooi, Cloetingh, & Burrus, 1992), but is consistent with 7.2 km predicted by Watts and Stewart (1998) for the Gabon passive margin. A relatively shallow depth of necking is appropriate for modeling the unloading of such a weak rifted margin. If actual necking is significantly deeper in the crust than we assume then our forward models will tend to underpredict the amplitude of rift flank uplift of the PRMB for any given elastic thickness (T_e).

5.4. Syn-rift subsidence

The predicted syn-rift stratigraphy and rift architecture using the flexural cantilever model for each of the four profiles analyzed are shown in Figs. 4–8(B). The predicted geometry of the basement is determined by extending a synthetic crustal section with a 15-km-thick brittle upper layer along each of the faults identified on the seismic sections. Planar fault geometry with an angle of 30° to the horizontal was assumed. Although the angles measured from the reflection seismic data ranged from 25 to 65°, the largest faults that accounted for most of the extension tended to have dips at the lower end of that range (Hayes et al., 1995). An original crustal thickness of 32 km was used, because this is the thickness of the crust close to the coast, away from the basin center, as measured by seismic refraction methods (Nissen et al., 1995). The resultant synthetic basin was filled with sediment to sea level in the case of the South China margin models. For the Dangerous Grounds margin, only 50% of accommodation space was filled in order to match the thicknesses of syn-rift sediment imaged. After filling with sediment the model section was then allowed to isostatically adjust, assuming a T_e of 3 km. Erosion was also applied to the subaerially exposed topography, with 80% of exposed terrain being removed prior to isostatic re-adjustment. The modeled profiles from the northern South China Sea margin show two or more sub-basins between the unrifted continental crust and an outer rise whose geometry changes markedly along strike. These model basins correspond to the center of the PRMB. No outer high is noted in the Dangerous Grounds models.

Using the flexural cantilever model and the degrees of upper crustal extension, the calculated whole crustal extension reaches β_{crust} of ~1.18 along Profile 1212, 1.37 along Profile 1554, 1.60 along Profile 1716, 1.20 along Profile SO-27-25 and 1.20 along Profile SO-23-29, less than predicted from the total amount of subsidence (Figs. 4–8(D)), or from the seismically determined crustal thickness close to Profile 1212. The implications of this mis-match are discussed below.

The modeled sections assume instantaneous extension while in reality extension lasts 9–19 Ma (Clift et al., 2001). This simplification introduces errors into the modeled sections because of the cooling of the lithosphere that occurs during the active extension. However, Jarvis and McKenzie (1980) have demonstrated that for extension lasting <20 my, the instantaneous extension model is not significantly different from one adjusted for the rift-duration. In any case slower extension will tend to reduce the post-rift subsidence and increase syn-rift subsidence, but should not strongly affect the total accommodation space or geometry of the basin, which are the principle data sets used in this study to compare model and observation.

5.5. Post-rift subsidence

The synthetic basins generated using the flexural cantilever model were then modified to incorporate the effects of post-rift subsidence, allowing direct comparison of the forward models and the interpreted profiles. The forward model employed assumes that the amount of post-rift thermal subsidence is controlled by the degree of ductile mantle lithospheric extension (Royden & Keen, 1980). Because the present South China Shelf typically has less than 100 m water depth landward of the shelf break, and because cored sediments in the PRMB show shallow water facies since the Oligocene (Clift and Lin, 2001), we forward modeled each synthetic section from this region assuming that a water depth of 100 m has been maintained since the end of extension at ~25 Ma. We know from well data that shallow marine (i.e. <250 m) conditions have prevailed on the shelf since initial transgression early in the post-rift thermal subsidence period, interspersed with occasional hiatuses, most notably at 11 Ma during the sea-level low-stand of that time (Haq, Hardenbol, & Vail, 1987; Miller, Fairbanks, & Mountain, 1987).

The assumption of constant shallow-water conditions is incorrect for the Dangerous Grounds, and because we have no drilling data to constrain paleo-water depths our forward model for those transects is less well controlled. Instead we chose to fill 50% of the accommodation space provided by the rifting because this amount of sedimentation produces sequence thicknesses close to those observed. Each model section was thus loaded with syn-and post-rift sediments, which are allowed to compact due to burial loading. In modeling sediment compaction, we used the cored lithologies identified from the wells, assuming that porosity can be described as an exponential function of depth (Ruby & Hubbert, 1960), $\phi = \phi_0 e^{-CZ,}$ where ϕ is porosity, Z depth below sealevel, ϕ_0 the porosity at the sediment surface, and C a controlling constant. For the lithologies of shale, sand

and limestone, we used values of 63, 49 and 70%, respectively, for ϕ_0, and 0.51, 0.27, and 0.71 km^{-1} for C, based on physical property measurements made at ODP wells in the South China Sea (Wang et al., 2000).

The modeling results in Figs. 4–8(C) are compared to the interpreted seismic sections of Figs. 4–8(A), with several important differences apparent. The total amount of predicted subsidence based on the flexural cantilever model and the associated post-rift subsidence is far less in all cases than observed. The forward models predicts that the outer rise that separates the PRMB from the continental slope should still be at sealevel (Figs. 4–6(C)). This prediction is in contrast to the observation that the outer rise is buried under ~2 km of post-rift sediment on profile 1554 (Fig. 5(A)), and under ~1 km in profiles 1212 (Fig. 4(A)) and 1716 (Fig. 6(A)). Basement depths across profiles SO-27-25 and SO23-29 are also shallower than observed, with the mis-fit increasing towards the COT.

Thus, it is clear that the flexural models based solely on the degrees of upper crustal brittle faulting and the assumed accompanying ductile but uniform extension at depth greatly underpredict the amount of post-rift thermal subsidence. This mis-match is especially severe on the oceanward side of each margin profile. Although some of the brittle faulting may not be imaged on the seismic profiles due to lack of fine-scale resolution, this alone will not account for the mis-match. Walsh, Watterson, and Yielding (1991) predict that as much as 40% of extension may not be imaged in reflection profiles. However, unless this missing extension was all concentrated over the outer structural high to the PRMB this will not help account for the mismatch. There is no reason to suspect that data quality or interpretation accuracy systematically decreases towards the continental slope. Fig. 11 shows a forward model for profile 1554 in which extension across each fault was artificially increased by 40%. This model assumes that the 'missing' extension is located in the regions where faulting has already been identified. The result of this correction is to increase the depth of the individual basins and thickness of the cover, but does not resolve the subsidence mis-match, which is largely the result of significant subsidence being observed in areas where there is no or little faulting. Although the missing 40% could hypothetically be placed in new faults near but not on the identified major faults this will not significantly change the amount of subsidence due to ductile lower crustal thinning, or due to postrift thermal subsidence which are both distributed over 100 km wavelengths around each fault.

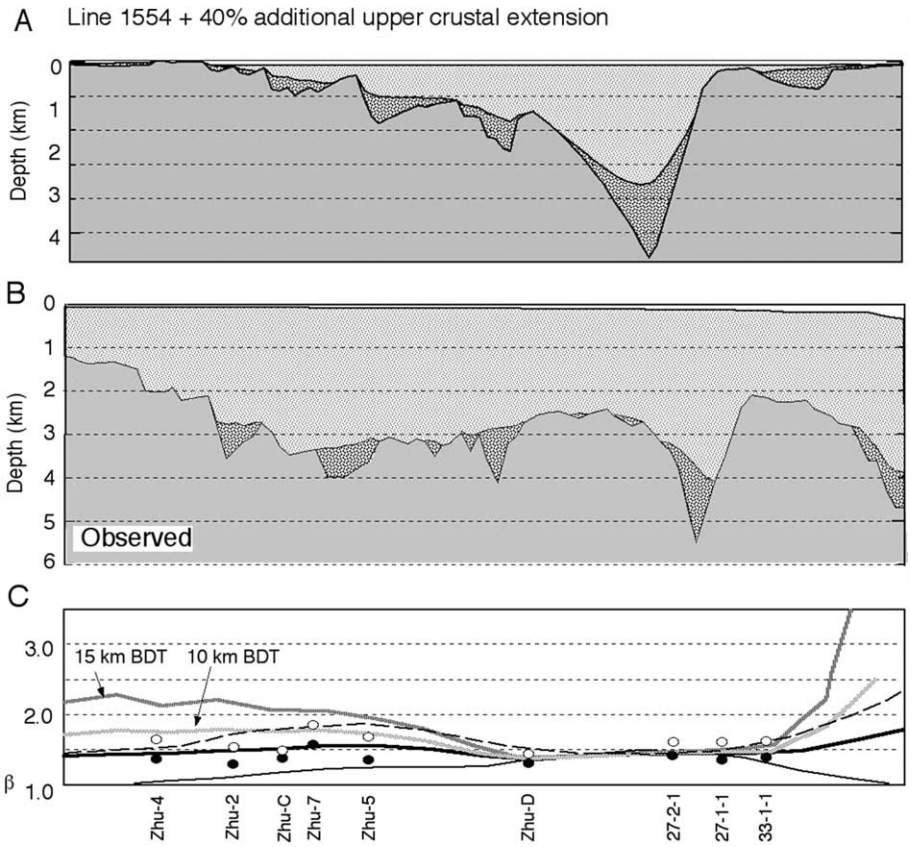

Fig. 11. (A) Forward flexural-cantilever model of profile 1554 28 my after rifting to show that even increasing extension by 40% across the section does not resolve the subsidence mis-match across the outer structural high. (B) Observed geometry of modern section. (C) Lateral variations in the predicted extension for the whole crust, upper crust, lower crust using the increased values for upper crustal extension. Solid dots and open circles represent, respectively, estimates of crustal and mantle extension derived from nearby wells projected on to the line of section.

5.6. Sensitivity to sea-level variation

The sensitivity of the basin models to the modeling parameters chosen can be quantified in order to assess whether variation in these values could account for some of the misfit between predictions and observations along the five profiles across the South China Sea margins. Sensitivity to T_e has been discussed above in Fig. 10. Variation in T_e would not generate subsidence across the entire section in the fashion required, but only change basin morphology locally.

In many subsidence studies no attempt is made to correct for fluctuations in eustatic sealevel, because current predictions of rates and magnitudes of eustatic sealevel remain controversial and would produce unlikely saw tooth-like subsidence curves when taken into account (Wood, 1982). Although short period sea-level fluctuations predicted by reconstructions like Haq et al. (1987) are difficult to account for, longer term variations may be incorporated without producing geologically impossible rifting histories. Haq et al. (1987) predict sealevel in the Early Cenozoic being about 150 m higher than today. However, predictions based on oxygen isotope work indicate sealevel during the Early Cenozoic only 30–50 m above modern levels (Miller, Mountain, & Tucholke, 1985), values supported by sequence stratigraphic studies of Atlantic passive margins (Clift, 1996; McGinnis, Driscoll, Karner, Brumbaugh, & Cameron, 1993). By accounting for Haq et al. (1987) sea-level reconstruction we see that the principal effect on the forward model section is to increase the elevation of the section at the present day, thus merely compounding rather than resolving the subsidence mis-fit.

6. Estimating crustal and mantle extension

Although the parameters of the extension model can be changed to vary the ratio of syn- and post-rift sediment, our synthetic sections based on this model and the observed faulting are unable to match the total sedimentary thicknesses measured in the seismic profiles. Along the PRMB profiles the mis-match between the cantilever model and observation is especially poor over the structural outer rise, where the lack of faulting in the upper crust indicates no upper crustal extension, but where significant post-rift subsidence has occurred. The same is true of the oceanward portion of the Dangerous Grounds profiles. The fact that there is significant post-rift subsidence close to the COT requires large-scale thinning of the crust, and in the absence of shallow crustal faulting implies that there must be preferential lower crustal thinning during active extension to account for the accommodation space created.

Once a model section has been generated it can then be compared with the modern observed section, allowing mismatches to be identified and interpreted in terms of departures of the extension patterns from that input and assumed by the model. Estimates of changing extension with depth in the plate can be made by considering different aspects of the subsidence history. Extension in the upper crust is estimated by summing the extension of the seismically observable faults, which forms the input to the flexural-cantilever forward model. Extension of the mantle lithosphere is estimated through the amount of post-rift thermal subsidence, after correcting the loading effects of the sediments and water, using the compaction parameters of Sclater and Christie (1980). Post-rift subsidence is normally considered to be purely thermally driven, i.e. due to conductive cooling and thickening of the lithosphere alone (McKenzie, 1978). Cooling of the crust represents a small fraction of this total effect, so that post-rift subsidence can be used as a proxy for mantle cooling and extension. Since water depth has been in the shallow shelf range since the end of rifting we use a value of 100 m as an average water depth. Uncertainty on the water depths will not seriously affect the mantle extension estimate because the sediment thicknesses are significantly greater than this value.

Total crustal extension is estimated from the amount of syn-rift subsidence, again after correcting for the sediment and water loading effect, as well as uplift driven by mantle thinning during rifting. Given the predicted background of mantle-driven uplift (calculated from the amount of post-rift subsidence) it is possible to calculate how much total crustal extension is needed to produce the net amount of subsidence observed. The shallow marine paleobathymetries of the syn-rift strata in the basin provide confidence that the syn-rift extension estimates have low uncertainties. Once total crustal extension has been derived from the total degree of accommodation space produced by rifting, the degree of lower crustal extension may be calculated by subtracting the upper crustal extension from the total crustal extension.

The combination of well and seismic data on the PRMB margin allows the degree of extension experienced by the mantle, and the upper and lower sections of the crust to be estimated. This comparison is especially instructive where refraction seismic information is available to independently constrain the total crustal thickness. In particular, profile 1212 lies close to deep-penetrating refraction profiles of Nissen et al. (1995), allowing comparison of two independent data sets. Along profile 1212 (Fig. 4(D)), the maximum upper crustal extension measured from faulting is $\beta_{\text{upper crust}} = 1.18$, while the total crustal extension measured from the maximum accommodation space on the profile and from nearby wells indicate total crustal extension of $\beta_{\text{crust}} = 1.4$ (Clift & Lin, 2001). Seismic refraction data give a modern crustal thickness of 22 km under the PRMB in this region, which when compared with the assumed original crustal thickness of 32 km yields a maximum $\beta_{\text{crust}} = 1.45$. Our estimates of total crustal extension derived from subsidence data are comparable to those from seismic refraction work. The upper crust appears to be always less extended than the total crust. This pattern of relatively small upper crustal extension is in accord with

the study of Westaway (1994) who calculated that the PRMB reaches a maximum $\beta_{\text{upper crust}}$ of 1.3, despite a total crustal extension of β_{crust} of 1.8.

6.1. Depth of faulting

As described above, given the total amount of crustal thinning, derived from the amount of accommodation space provided across the margin, and an estimate of the extension in the brittle upper crust, it is possible to calculate the amount of extension required in the lower crust for a mass balance to be achieved. For this calculation we must assume a depth to the brittle–ductile transition. For continental lithosphere with a quartz-dominated rheology and a geothermal gradient of 15–18 °C/km, this transition is usually estimated as lying between 10 and 15 km (Zuber, Parmentier, & Fletcher, 1986), a range supported by the observed depth of seismic activity in most rifts (Bufe, Horsh, & Burford, 1977; Kusznir and Park, 1984), although seismicity is noted at >25 km in rifted cratons, such in the East African and Baikal rifts (Foster & Jackson, 1998; Jackson & Blenkinsop, 1995). In the case of the South China lithosphere its history as an active margin during the Mesozoic makes comparison with the cold, thick lithosphere of a craton inappropriate, and so we consider the brittle–ductile transition to lie at 10–15 km at the start of extension. Given the measured geothermal gradient of 83 °C/km at ODP Site 1148 (Clift et al., 2001) the transition may in fact be somewhat shallower than even 10 km. We use 10–15 km as the depth to the brittle–ductile transition. Although this seems to be at odds with the reflection seismic observation of faults cutting the entire crust (Hayes et al., 1995), it is noteworthy that of the five penetrating faults recorded, all but one occur in regions where the crustal thickness is <15 km, implying that extension has proceeded so far in these places that the ductile lower crust has been completely removed. Extension could therefore initially have been ductile in the lower crust, until the point that this layer was preferential extended to zero thickness. At that stage the brittle upper crust lay directly on the Moho, producing the relationships observed by Hayes et al. (1995). This scenario would be consistent with the extensional models of Pérez-Gussinyé, Reston, Phipps, and Morgan (2001), who showed that as extension proceeds ductile weak zones within the crust become thinner until the entire crust is affected by brittle faulting. The rate at which brittle faulting advance depends on the heatflow, extension rate and original crustal thickness. In this study we calculate extension in the lower crust for both depths of faulting of 10 and 15 km in order to assess the range of reasonable extension values at this crustal level (Figs. 4–8(D)).

6.2. Evidence for lower crustal flow

The location of wells within, and seismic profiles through, the PRMB allows the maximum mantle extension in the basin center to be estimated independently. β_{mantle} does not exceed 1.8 (Clift & Lin, 2001; Su et al., 1989), which is less than that inferred for $\beta_{\text{lower crust}}$ if the brittle–ductile transition is assumed to be at 15 km depth, but about the same if 10 km is a more reasonable estimate for Profile 1554 (Fig. 5). There is no reason why the lower crust should not extend more than the lithospheric mantle, since its quartz-dominated lithologies makes it weaker at typical lower crustal temperatures and pressures, compared to the olivine-dominated upper mantle (Kirby & Kronenberg, 1987; Kohlstedt & Goetze, 1974; Sonder & England, 1989). Modeling by Hopper and Buck (1998) shows that lower crustal flow might be expected for a range of heatflow values when the continental crust is 30 km thick, and when quartz is the dominant mineralogy, as is likely here. Finite-element theoretical models of passive margin formation (e.g. Baltimore Canyon Trough; Sawyer & Harry, 1991) have predicted an oceanward flow of lower crustal material from under opposing conjugate margins. If this flow did occur then this material must be present oceanward of the extended upper crust and mantle, and implies a weak, low viscosity lower crust.

Along Profile 1554 (Fig. 5), no seismic refraction data is available, but estimates of the total crustal extension may be made from the total accommodation space. In order to directly compare the extension estimates based on modeling of seismic sections with those derived from drilling data (Clift & Lin, 2001), the mantle and whole crustal extension estimates from nearby wells are projected along strike on to the section in Fig. 5. In calculating $\beta_{\text{lower crust}}$ across the PRMB there is no attempt to conserve the original volume of lower crust. Instead our calculations only require that the lower and upper crustal extension in any given place results in a net extension equal to that derived for the total crust. As a result lower crust can be lost from the section if it extends more than the upper crust.

Upper crustal extension in the central PRMB along Profile 1554 rises to $\beta_{\text{uppercrust}} = 1.13$, reaching a maximum $\beta_{\text{upper crust}} = 1.31$ in a major half graben adjacent to the structural outer rise (Fig. 5(D)). Analysis of the tectonic subsidence at the nearby wells implies maximum total crust $\beta_{\text{crust}} = 1.45$ near the outer structural high, and $\beta_{\text{crust}} = 1.32–1.38$ in the central basin. Since $\beta_{\text{upper crust}} = 1.31$ under the outer rise, this implies $\beta_{\text{lower crust}}$ of at least 1.60 in order to conserve mass, assuming that the faulting only affects the upper 15 km. In this case $\beta_{\text{lower crust}}$ value is close to β_{mantle} values derived from modeling the backstripped histories at each well ($\beta_{\text{mantle}} = 1.65$; Clift & Lin, 2001). Well control is insufficient to make such detailed comparisons along profiles SO-27-25 and SO-23-29 on the Dangerous Grounds margin. Here extension estimates must be derived from the thicknesses of the syn- and post-rift strata, together with the water depth. The reliability of such estimates is less than that derived from the PRMB, but the overall pattern of extension is similar to that seen along the other profiles.

6.3. Implications for strain accommodation on conjugate margins

The estimates of extension discussed above are not in agreement with a pure shear model of continental extension in which all levels of the plate are extended to the same degree (McKenzie, 1978). Although the greater extension in the lower crust and mantle relative to the upper crust raises the question as to whether the South China Shelf (Figs. 4–6) might represent the upper plate in a simple shear system, the Dangerous Grounds profiles eliminate this as a possibility. Earlier studies of the rift architecture on Dangerous Grounds margin indicate that there is a consistent northward-dipping sense to the listric faulting, some of which seems to shallow into sub-horizontal detachment surfaces (Schlüter et al., 1996). This geometry was interpreted to represent typical characteristics of a lower plate to a simple shear system. Our subsidence modeling demonstrates that this interpretation is not self-consistent, since this margin also experiences preferential lower crustal extension that increases towards the COT. The result from Dangerous Grounds is consistent with the earlier results from Nan Con Som Basin and the South China margin by Clift et al. (2001) in showing uniform preferential thinning of the lower crust adjacent to the COT.

The fact that both conjugate margins have experienced preferential lower crustal thinning means that the lower crust removed from under one margin is not located under the opposing margin. The density difference with the mantle precludes this material from flowing landward under the thicker crust of the continental interior, and instead favors its loss and incorporation into the oldest 'spread' oceanic crust. Clift et al. (2001) showed that lower crustal thinning occurred in the Nan Con Som Basin, positioned ahead of the South China Sea propagating spreading axis during the Miocene. Thus, although lower crustal material could not be lost from both conjugate margins without the onset of seafloor spreading, as there would be nowhere for the ductile crust to flow to, this process does seem to slightly pre-date the spreading itself. Evidence for the flow of lower crustal material into the oldest oceanic crust should be identifiable by shallower than normal basement depths close to the COT and the geochemical contamination of the pure mid ocean ridge basalt character. At this time we do not have data to test these model predictions. It is noteworthy that in the Beibu Gulf Basin, which is not adjacent to COT (Fig. 1), Clift et al. (2001) did not find any evidence for basinwide loss of lower crust using the same methodology. We can thus infer that our conclusion of lower crust loss along the margins of the South China Sea, adjacent to the COT, is not simply the product of our methodology or the nature of the crust in southern China.

The strain measured across both conjugate margins is consistent with a depth-dependent extension, or both

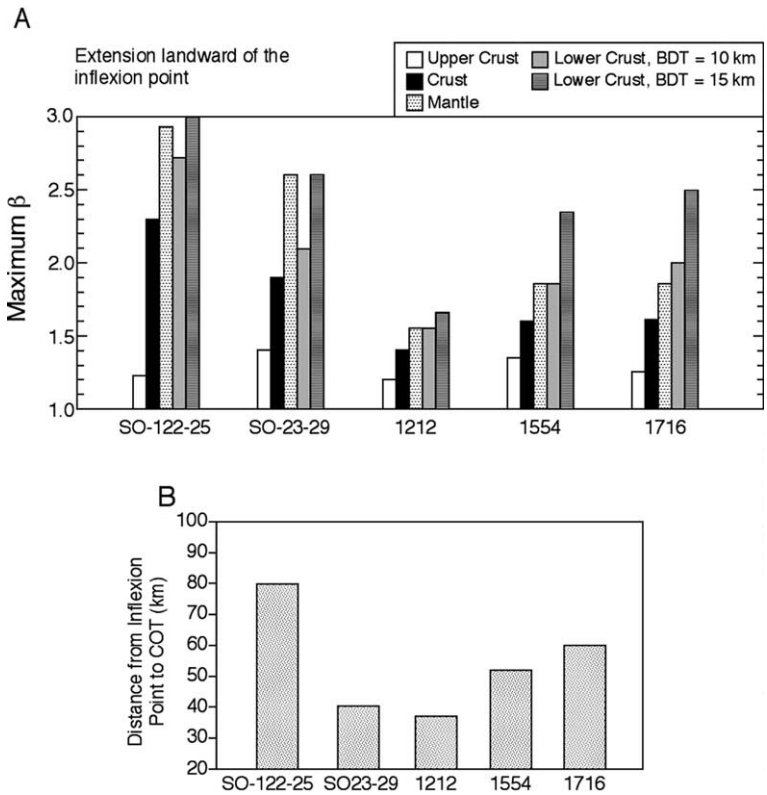

Fig. 12. (A) Comparison of the amount of extension at different levels in the continental lithosphere landward of the inflexion point beyond which extension rapid increases towards the COT. (B) Comparison of the distance from the inflexion points to the oldest oceanic crust for the four profiles considered in this study.

the landward-dipping detachments and preferential lower crust thinning proposed by Driscoll and Karner (1998). Comparisons of the different degrees of extension at different lithospheric levels along each of the five transects considered here are shown in Fig. 12. The diagram only considers those portions of the profiles that lie landward of the inflexion point beyond which extension rises rapidly towards the COT (Figs. 4–8). Maximum degrees of upper crustal extension vary from $\beta_{\text{upper crust}}$ of 1.2–1.4 for all sections. Mantle extension exceeds total crustal extension in all sections, independently confirming the results of the backstripping study of Clift and Lin (2001). The Dangerous Grounds profiles and the eastern PRMB profiles show the greatest preferential thinning of the lower crust compared to the upper crust.

There is also a systematic change in extensional style from west to east along the South China margin, with Profile 1212, which lies at the western end of the PRMB, showing a relative short distance between inflexion point and COT, and only moderate preferential thinning of the lower crust. In contrast, the eastern PRMB show generally greater distances between inflexion point and COT, and a marked preferential thinning of the lower crust.

7. Viscosity of the lower crust

The overall shape of the rifted margin can be used to infer the viscosity of the lower crust. Many workers have proposed that in regions of high heat flow the low viscosity

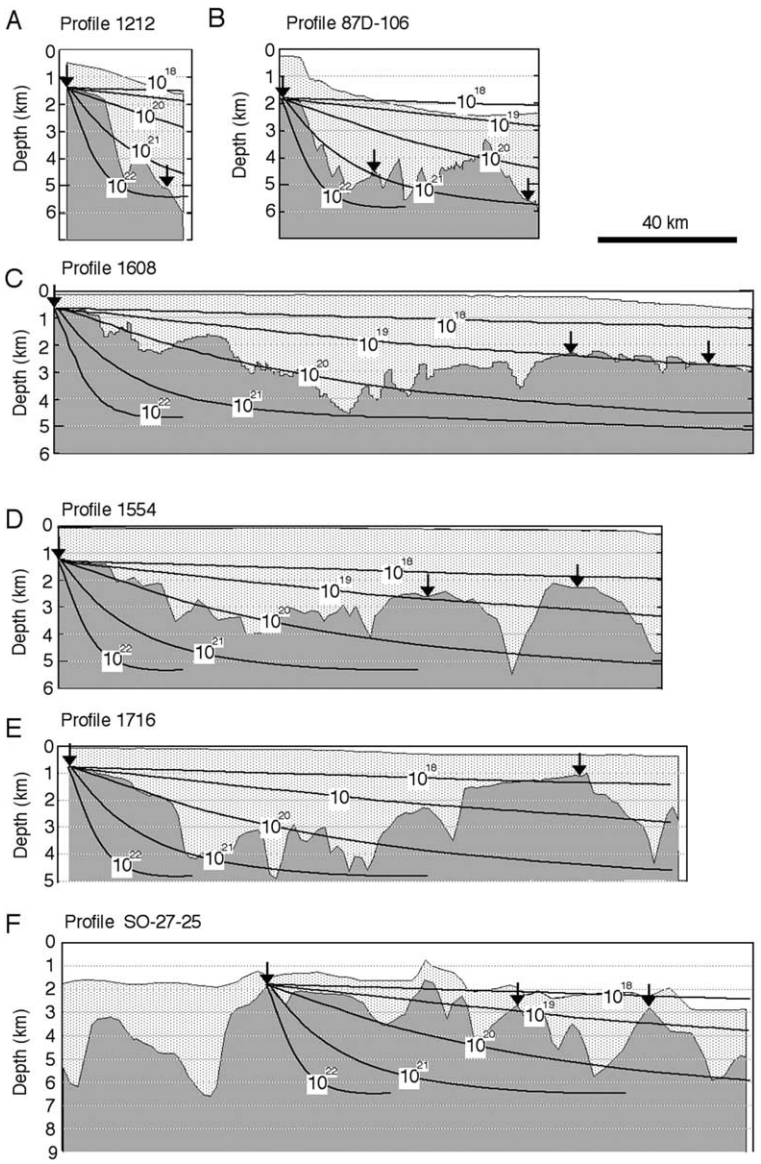

Fig. 13. Predicted topographic profiles for crust assuming a viscous lower crustal channel 15 km thick and with variable viscosity, labeled in units of Pa s. Model from Clark and Royden (2000). Arrows indicate arbitrarily defined reference points on the basement surface that help define the overall slope of the margin, outside the local influence of small scale basins and blocks.

of the lower crust allows it to flow and so equilibrate lateral pressure gradients (Bird, 1991; Block & Royden, 1990; Wdowinski & Axen, 1992). Such flow acts to reduce variation in topography and crustal thicknesses. The long wavelength topographic gradient can thus be used to infer the viscosity of the lower crust. We here compare our margin profiles with the model of Clark and Royden (2000) in which flow in the lower crust is modeled as a 15-km-thick channel. Although Wernicke (1990) suggested a range of 5–25 km for such lower crustal channels, 15 km is appropriate given estimates of the ductile layer under the South China Margin (10–15 km) and the total crustal thickness (~30–18 km). The predicted basin profiles for a variety of viscosities are shown in Fig. 13 against the South China Sea margins modeled above, as well as one profile from the western part of the margin, south of Hainan (Profile 87D-106; Fig. 2), and the long profile 1608 modeled by Clift et al. (2001). Palawan profile SO-23-29 is not considered because the rough basement surface, shorter length and probable flexural deformation at the southern end make comparison difficult. Ideally the basement topography would be averaged over wider areas of the margin in order to filter out short wavelength features created by local faulting, but this is not practical unless many seismic profiles were available to be interpreted. Averaging the margin profile is preferred because we wish to compare the overall slope of the margin in different places and the model profiles, which are necessarily smooth. In Fig. 13 we highlight the tie points which we consider to best represent the gradient of the margin without being strongly affected by local block faulting, although the choices of such tie points are not unique.

The bathymetry in Fig. 2 provides a general guide to how modern lower crustal viscosity varies because areas of low viscosity and high heatflow are unable to support steep topographic gradients over geological time-scales. In this case, the steep margin slopes south of Hainan contrast with the gentle slopes towards the east, suggesting more viscous lower crust under Hainan than in the main PRMB, Indeed the very existence of Hainan, representing a body of unrifted crust in a region where equivalent crust to east and west along the margin is extended, is suggestive of a more rigid block in an environment of otherwise more fluid lower crust.

Estimates of the lower crustal viscosity during rifting can be assessed by looking at the long-wave length slope to the basement topography. While faulting generates many small wavelength sub-basins that are not predicted by the viscosity model, the overall slope of the basement between the landward structural high and the unfaulted outer rise in the PRMB does permit the effect of lower crustal viscosity to be determined. Mirroring the overall topography of the seafloor, the western South China margin basement shows steeper slopes and thus higher viscosities of 10^{22}–10^{21} Pa s. In the central and eastern South China margin, and the Dangerous Grounds, viscosities are much lower and range between 10^{18} and 10^{19} Pa s. This is a relatively low figure, comparable to the 10^{18} Pa s estimated by Clark and Royden (2000) for the eastern margin of the Tibetan Plateau. This result is compatible with the model of a weak lower crust to the South China Margin derived from the subsidence modeling, discussed above. Furthermore, it suggests that South China Margin should be considered as part of larger system of weak lower crust that underlies much of Tibet and southern China.

8. Conclusions

Forward modeling of basin geometry based on the faulting in the brittle upper crust alone on the South China and Dangerous Grounds conjugate margins is incapable of reproducing the observed basement topography. Present-day flexural deformation of the Dangerous Grounds into the Palawan Trough indicates modern values of T_e not exceeding 10 km, while a T_e of 13 km is preferred for the South China Shelf close to Taiwan (Lin & Watts, 2002). Flexural rigidity is presumed to have been less during active extension, prior to ~25 Ma. Whatever value of T_e is used the uniform extension assumption within the extension model used here means that forward models of both margins do not predict sufficient subsidence to match observations on either conjugate margin, especially towards the COT. This prediction does not change even if faulting below the resolution of seismic techniques is accounted for. Our results demonstrate preferential extension of the lower crust on both margins extending as much as 80 km from the COT, especially in the eastern part of the South China margin and under the Dangerous Grounds. Lower crustal thinning by flow from over both conjugate margins towards the oceanic crust of the South China Sea is predicted. This flow must have taken place just prior to and during the offset of seafloor spreading. The low overall modern slope of the South China Sea passive margin and its pre-rift basement implies that lower crustal viscosities are low and were low during continental break-up (10^{18} and 10^{19} Pa s), except in the region of Hainan Island. The western South China margin represents a harder viscous block within a region of weak, flowing lower crust. Thus the South China Sea can be seen to be part of a greater weak crustal zone in eastern Asia, forming an offshore extension of the crustal flow documented on the eastern flank of the Tibetan Plateau.

Acknowledgements

The data used in this study was released by an agreement with the Chinese National Offshore Oil Company (CNOOC), BP Exploration Operating Company Ltd. and the Department of Energy, Government of the Philippines. We are grateful to Richard Miller and David Roberts at BP Exploration in Sunbury-on-Thames, UK, and to Ismael Ocampo in Manila for their generous help in providing data

for this study. Alan Roberts, Mark Davis, and Nick Kusznir are thanked for their help with the STRETCH™ software package. Nicky White is thanked for his comments on an earlier version of this paper. PC thanks Marta Pérez-Gussinyé for her advice and comments on ideas expressed here. The manuscript was improved by comments from two anonymous reviewers. This work was supported by the US Naval Oceanographic Office, Office of Naval Research, National Science Foundation and the Woods Hole Oceanographic Institution. This is WHOI contribution number 10814.

References

Barton, P., & Wood, R. (1984). Tectonic evolution of the North Sea Basin: crustal stretching and subsidence. *Geophysical Journal of the Royal Astronomical Society*, *79*, 987–1022.

Behn, M. D., Lin, J., & Zuber, M. T. (2002). A continuum mechanics model for normal faulting using a strain-rate softening rheology: Implications for thermal and rheological controls on continental and oceanic rifting. *Earth and Planetary Science Letters*, *202 (3–4)*, 725–740.

Bellingham, P., & White, N. J. (2000). A general inverse method for modelling extensional sedimentary basins. *Basin Research*, *12*, 219–226.

Bird, P. (1991). Lateral extrusion of lower crust from under high topography, in the isostatic limit. *Journal of Geophysical Research*, *96*, 10,275–10,286.

Block, L., & Royden, L. H. (1990). Core complex geometries and regional scale flow in the lower crust. *Tectonics*, *9*, 557–567.

Boillot, G., Beslier, M. O., Krawczyk, C. M., Rappin, D., Reston, T. J., et al. (1995). The formation of passive margins: constraints from the crustal structure and segmentation of the deep Galicia margin, Spain. R. A.Scrutton, *Geological Society of London, Special Publication*, *vol. 90*, 71–91.

Briais, A., Patriat, P., & Tapponnier, P. (1993). Updated interpretation of magnetic anomalies and seafloor spreading stages in the South China Sea: implication for the Tertiary tectonics of southeast Asia. *Journal of Geophysical Research*, *98*, 6299–6328.

Buck, W. R. (1988). Flexural rotation of normal faults. *Tectonics*, *7*, 959–973.

Buck, W. R. (1991). Modes of continental lithospheric extension. *Journal of Geophysical Research*, *96*, 20,161–20,178.

Bufe, C. G., Horsh, P. W., & Burford, R. O. (1977). Steady-state seismic slip—precise recurrence model. *Geophysical Research Letters*, *4*, 91–94.

Carter, N. L. (1976). Steady state flow of rocks. *Reviews of Geophysics and Space Physics*, *14*, 301–360.

Clark, M. K., & Royden, L. H. (2000). Topographic ooze: building the eastern margin of Tibet by lower crustal flow. *Geology*, *28*, 703–706.

Clift, P. D., Lin, J., ODP Leg 184 Scientific Party (2001). Patterns of extension and magmatism along the continent–ocean boundary, South China margin. In: Non-volcanic rifting of continental margins: a comparison of evidence from land and sea (Ed. by R. C. Wilson, R. B. Whitmarsh, B. Taylor, & N. Froitzheim), *Geological Society, London, Special Publication*, *187*, 489–510.

Clift, P. D., & Lin, J. (2001). Preferential mantle lithospheric extension under the South China margin. *Marine and Petroleum Geology*, *18*, 929–945.

Clift, P. D. (1996). Plume tectonics as a cause of mass wasting on the southeast Greenland continental margin. *Marine and Petroleum Geology*, *13*, 771–780.

Davis, D. W., Sewell, R. J., & Campbell, S. D. G. (1997). U–Pb dating of mesozoic igneous rocks from Hong Kong. *Journal of the Geological Society, London*, *154*, 1067–1076.

Draut, A. E., Clift, P. D., Hannigan, R., Layne, G. D., & Shimizu, N. (2002). A model for continental crust genesis by arc accretion: rare earth element evidence from the Irish caledonides. *Earth and Planetary Science Letters*, *203 (3–4)*, 861–877.

Driscoll, N. W., & Karner, G. D. (1998). Lower crustal extension across the Northern Carnarvon basin, Australia: evidence for an eastward dipping detachment. *Journal of Geophysical Research*, *103*, 4975–4991.

Ebinger, C. J., Bechtel, T. D., Forsyth, D. W., & Bowin, C. O. (1989). Effective elastic plate thickness beneath the East African and Afar plateaus and dynamic compensation of the uplifts. *Journal of Geophysical Research*, *94*, 2883–2901.

Eldholm, O., Skogseid, J., Planke, S., & Gladczenko, T. (1995). Volcanic margin concepts. In E. Banda, et al. (Eds.), *Rifted ocean–continent boundaries* (pp. 1–16). Dordrecht: Kluwer.

England, P. C., & Houseman, G. A. (1988). The mechanics of the Tibetan Plateau. *Philosophical Transactions of the Royal Society, London, Series A*, *326*, 301–320.

Foster, A. N., & Jackson, J. A. (1998). Source parameters of large African earthquakes; implications for crustal rheology and regional kinematics. *Geophysical Journal International*, *134*, 422–448.

Fowler, S., & McKenzie, D. P. (1989). Gravity studies of the Rockall and Exmouth Plateau using SEASAT altimetry. *Basin Research*, *2*, 27–34.

Hamilton, W. (1979) (*Vol. 1087*). *Tectonics of the Indonesian region, Geological Survey Paper*, Washington, DC: US Government Printing Office, pp. 0–345.

Haq, B. U., Hardenbol, J., & Vail, P. R. (1987). Chronology of fluctuating sea levels since the Triassic. *Science*, *235*, 1156–1167.

Hayes, D. E., Nissen, S., Buhl, P., Diebold, J., Bochu, Y., Weijun, Z., & Yongqin, C. (1995). Through-going crustal faults along the northern margin of the South China Sea and their role in crustal extension. *Journal of Geophysical Research*, *100*, 22,435–22,446.

Hinz, K., & Schlüter, H.-U. (1985). Geology of the dangerous grounds, South China Sea, and the continental margin off southwest Palawan: results of Sonne cruises SO23 and SO-27. *Energy*, *10*, 297–315.

Hirth, G., & Kohlstedt, D. L. (1996). Water in the oceanic upper mantle; implications for rheology, melt extraction and the evolution of the lithosphere. *Earth and Planetary Science Letters*, *144*, 93–108.

Hopper, J. R., & Buck, W. R. (1998). Styles of extensional decoupling. *Geology*, *26*, 699–702.

Jackson, J., & Blenkinsop, T. (1993). The Malawi earthquake of March 10, 1989; deep faulting within the East African Rift system. *Tectonics*, *12*, 1131–1139.

Jahn, B., Chen, P. Y., & Yen, T. P. (1976). Rb–Sr ages of granitic rocks from southeastern China and their tectonic significance. *Bulletin of the Geological Society of America*, *87*, 763–776.

Janssen, M. E., Torne, M., Cloetingh, S., & Banda, E. (1993). Pliocene uplift on the eastern Iberian margin; inference from quantitative modeling of the Valencia Trough. *Earth and Planetary Science Letters*, *119*, 585–597.

Jarvis, G. T., & McKenzie, D. P. (1980). Sedimentary basin formation with finite extension rates. *Earth and Planetary Science Letters*, *48*, 42–52.

Karner, G. D., & Watts, A. B. (1982). On isostasy at Atlantic-type continental margins. *Journal of Geophysical Research*, *87*, 2923–2948.

Kelemen, P. B., & Holbrook, W. S. (1995). Origin of thick high-velocity igneous crust along the US east coast margin. *Journal of Geophysical Research*, *100*, 10,077–10,094.

Kirby, S. H., & Kronenberg, A. K. (1987). Rheology of the lithosphere: selected topics. *Reviews in Geophysics*, *25*, 1219–1244.

Kohlstedt, D. L., & Goetze, C. (1974). Low-stress high-temperature creep in olivine single crystals. *Journal of Geophysical Research*, *79*, 2045–2051.

Kooi, H., Cloetingh, S. A. P. L., & Burrus, J. (1992). Lithospheric necking and regional isostasy at extensional basins; 1 subsidence and gravity modeling with an application to the Gulf of Lions margin (SE France). *Journal of Geophysical Research*, *97*, 17,553–17,571.

Kusznir, N. J., & Egan, S. S. (1989). Simple-shear and pure-shear models of extensional sedimentary basin formation: Application to the Jean D'Arc

basin, Grand Banks of Newfoundland. A. J.Tankard, H. R.Balkwill, *American Association of Petroleum Geologists, Memoir*, *46*, 305–322.

Kusznir, N. J., & Park, R. G. (1984). Intraplate lithospheric deformation and the strength of the lithosphere. *Geophysical Journal of the Royal Astronomical Society*, *70*, 513–538.

Kusznir, N. J., Marsden, G., Egan, S. S. (1991). A flexural cantilever simple shear/pure shear model of continental extension. A. M.Roberts, *Geological Society, London, Special Publication*, *Vol. 56*, 41–61.

Kusznir, N. J., Roberts, A. M., & Morley, C. K. (1995). Forward and reverse modelling of rift basin formation. J. J.Lambiase, *Geological Society, London, Special Publication*, *Vol. 80*, 33–56.

Lee, T. Y., Lo, C. H., Chung, S. L., Lan, C. Y., Wang, P. L., & Lee, J. C. (1999). Cenozoic tectonics of the South China continental margins and the opening of the South China Sea. *Eos Transactions AGU*, *80* Fall Meeting Supplement, 1042.

Lin, A. T.-S., & Watts, A. B. (2002). Origin of the West Taiwan basin by orogenic loading and flexure of a rifted continental margin. *Journal of Geophysical Research*, *107 (B9)*, 2185.

Lithgow-Bertelloni, C., & Gurnis, M. (1997). Cenozoic subsidence and uplift of continents from time-varying dynamic topography. *Geology*, *25*, 735–738.

Lu, W., Ke, C., Wu, J., Liu, J., & Lin, C. (1987). Characteristics of magnetic lineations and tectonic evolution of the South China Sea basin. *Acta Oceanologica Sinica*, *6*, 577–588.

Maggi, A., Jackson, J. A., McKenzie, D. P., & Priestley, K. (2000). Earthquake focal depths, effective elastic thickness, and the strength of the continental lithosphere. *Geology*, *28*, 495–498.

McGinnis, J. P., Driscoll, N. W., Karner, G. D., Brumbaugh, W. D., & Cameron, N. (1993). Flexural response of passive margins to deep-sea erosion and slope retreat: implications for relative sea-level change. *Geology*, *21*, 893–896.

McKenzie, D. P. (1978). Some remarks on the development of sedimentary basins. *Earth and Planetary Science Letters*, *40*, 25–32.

Miller, K. G., Fairbanks, R. G., & Mountain, G. S. (1987). Tertiary oxygen isotope synthesis, sea level history, and continental margin erosion. *Paleoceanography*, *2*, 1–19.

Miller, K. G., Mountain, G. S., & Tucholke, B. E. (1985). Oligocene glacio-eustacy and erosion on the margins of the North Atlantic. *Geology*, *13*, 10–13.

Nissen, S. S., Hayes, D. E., Buhl, P., Diebold, J., Bochu, Y., Weijun, Z., & Yongqin, C. (1995). Deep penetration seismic soundings across the northern margin of the South China Sea. *Journal of Geophysical Research*, *100*, 22,407–22,433.

Pérez-Gussinyé, M., Reston, T., Phipps Morgan, J. (2001). Serpentinized and magmatism during extension at non-volcanic margins—effects of initial lithosphere structure. In: *Non-volcanic rifting of continental margins: a comparison of evidence from land and sea* (Ed. by R. C. Wilson, R. B. Whitmarsh, B. Taylor, & N. Froitzheim), *Geological Society, London, Special Publication*, *187*, 551–576.

Roberts, A. M., & Kusznir, N. J. (1998). Comments on flank uplift and topography at the central Baikal Rift (SE Siberia): a test of kinematic models for continental extension by Peter van der Beek. *Tectonics*, *17*, 322–323.

Roberts, A. M., Yielding, G., Kusznir, N. J., Walker, I., & Dorn-Lopez, D. (1993). Mesozoic extension in the North Sea: constraints from flexural backstripping, forward modelling and fault populations. J. R.Parker, *Proceedings of the Fourth Conference, Geological Society, London*, 1123–1136.

Royden, L., & Keen, C. E. (1980). Rifting processes and thermal evolution of the continental margin of eastern Canada determined from subsidence curves. *Earth and Planetary Science Letters*, *51*, 714–717.

Ruby, W. W., & Hubbert, M. K. (1960). Role of fluid pressure in the mechanics of overthrust faulting, II, overthrust belt in geosynclinal area of western Wyoming in light of fluid pressure hypothesis. *Bulletin of the Geological Society of America*, *60*, 167–205.

Sawyer, D. S., & Harry, D. L. (1991). Dynamic modeling of divergent margin formation; application to the US Atlantic margin. *Marine Geology*, *102*, 29–42.

Schlüter, H. U., Hinz, K., & Block, M. (1996). Tectono-stratigraphic terranes and detachment faulting of the South China Sea and Sulu Sea. *Marine Geology*, *130*, 39–78.

Sclater, J. G., & Christie, P. A. F. (1980). Continental stretching: an explanation of the post Mid-Cretaceous subsidence of the central North Sea basin.. *Journal of Geophysical Research*, *85*, 3711–3739.

Sonder, L. J., & England, P. C. (1989). Effects of a temperature-dependent rheology on large-scale continental extension. *Journal of Geophysical Research*, *94*, 7603–7619.

Su, D., White, N., & McKenzie, D. (1989). Extension and subsidence of the Pearl River mouth basin, northern South China Sea. *Basin Research*, *2*, 205–222.

Taylor, B., & Hayes, D. E. (1980). The tectonic evolution of the South China Basin. D. E.Hayes, *American Geophysical Union, Geophysical Monograph*, *23*, 89–104.

Van der Beek, P. (1997). Flank uplift and topography at the central Baikal Rift (SE Siberia): a test of kinematic models for continental extension. *Tectonics*, *16*, 122–136.

Van der Beek, P. (1998). Reply to comments on flank uplift and topography at the central Baikal Rift (SE Siberia): a test of kinematic models for continental extension. *Tectonics*, *17*, 324–327.

Walsh, J., Watterson, J., & Yielding, G. (1991). The importance of small-scale faulting in regional extension. *Nature*, *351*, 391–393.

Wang, P., Prell, W. L., Blum, P., Arnold, E. M., Buehring, C. J., Chen, M-P., Clemens, S. C., Clift, P. D., Colin, C. J. G., Farrell, J. W., Higginson, M. J., Jian Zhimin., Kuhunt, W., Laj, C. E., Lauer-Leredde, C., Leventhal, J. S., Li, A., Li, Q., Lin, J., McIntyre, K., Miranda, C. R., Nathan, S. A., Shyu, J-P., Solheid, P. A., Su, X., Tamburini, F., Trentesaux, A., Wang, L. (2000). *Proceedings of the Ocean Drilling Program, Initial Reports, 184*. Ocean Drilling Program, College Station, TX.

Watts, A. B. (1988). Gravity anomalies, crustal structure and flexure of the lithosphere at the Baltimore Canyon Trough. *Earth and Planetary Science Letters*, *89*, 221–238.

Watts, A. B., & Stewart, J. (1998). Gravity anomalies and segmentation of the continental margin offshore West Africa. *Earth and Planetary Science Letters*, *156*, 239–252.

Wdowinski, S., & Axen, G. J. (1992). Isostatic rebound due to tectonic denudation; a viscous flow model of a layered lithosphere. *Tectonics*, *11*, 303–315.

Weissel, J. K., & Karner, G. D. (1989). Flexural uplift of rift flanks due to mechanical unloading of the lithosphere during extension. *Journal of Geophysical Research*, *94*, 13,919–13,950.

Wernicke, B. P. (1990). The fluid crustal layer and its implications for continental dynamics. In M. H. Salisbury, & D. M. Fountain (Eds.), *Exposed cross-sections of the continental crust* (pp. 509–544). *NATO ASI Series*, Dordrecht: Kluwer.

Westaway, R. (1994). Re-evaluation of extension across the Pearl River Mouth Basin, South China Sea: implications for continental lithosphere deformation mechanisms. *Journal of Structural Geology*, *16*, 823–838.

Wheeler, P., & White, N. (2000). Quest for dynamic topography: observations from Southeast Asia. *Geology*, *28*, 963–966.

White, R. S. (1999). The lithosphere under stress. *Philosophical Transactions, Royal Society. Mathematical, Physical and Engineering Sciences*, *357*(1753), 901–915.

Wood, R. J (1982). *Subsidence in the North Sea*. Unpublished PhD Thesis, Cambridge University, England.

Zuber, M. T., Parmentier, E. M., & Fletcher, R. C. (1986). Extension of continental lithosphere: a model for two scales of basin and range deformation. *Journal of Geophysical Research*, *91*, 4826–4838.